Recycling of fines from waste concrete: development of lightweight masonry blocks and assessment of their environmental benefits

V. Nežerka[a,*], Z. Prošek[b,a], J. Trejbal[a], J. Pešta[b,c], J. A. Ferriz-Papi[d], P. Tesárek[a]

[a]*Faculty of Civil Engineering, Czech Technical University in Prague, Thákurova 7, 166 29 Praha 6, Czech Republic*
[b]*University Center for Energy Efficient Buildings, Czech Technical University in Prague, Třinecká 1024, 273 43 Buštěhrad, Czech Republic*
[c]*Faculty of Environmental Technology, University of Chemistry and Technology Prague, Technická 5, 166 28 Praha 6, Czech Republic*
[d]*University of Salford, 43 Crescent, Salford M5 4WT, United Kingdom*

Abstract

A significant body of research has been carried out to find suitable waste materials or industrial by-products that could replace portland cement and reduce the environmental footprint of the concrete industry. Many studies focus on technical aspects, lacking an assessment of environmental impacts associated with using these alternative materials, and the contribution to the sustainability of the sector remains unclear. In this paper, we present the development of lightweight blocks containing the finest fractions of waste concrete along with a holistic study of the developed product's structural and environmental performance. The results demonstrate the feasibility of such a recycling strategy and its environmental benefits. However, despite replacing 60 wt.% of portland cement in the developed lightweight blocks, their carbon footprint is not negligible, and to reduce CO_2 emissions in the construction sector significantly will require holistic measures that promote the reuse of whole building elements instead of their disintegration and subsequent recycling.

Keywords: Construction and demolition waste, LCA, Recycling, Masonry blocks, Aerated concrete

---

*Corresponding author
Email address: `vaclav.nezerka@fsv.cvut.cz` (V. Nežerka)

Nomenclature

CDW	Construction and demolition waste
PC	Portland cement
SCMs	Supplementary cementitious materials
RCF	Recycled concrete fines
LCA	Life-cycle assessment
AAC	Aerated autoclaved concrete
MFs	Microfibers
SP	Superplasticizer
FA	Foaming agent
XRF	X-ray fluorescence spectroscopy
C_3S	Tricalcium silicate (alite)
C_3A	Tricalcium aluminate
C_2S	Dicalcium silicate (belite)
LOI	Loss on ignition
PP	Polypropylene
w/c	Water-to-cement ratio
ρ_{b}	Bulk density
FTR	Flow test result
$E_{\mathrm{dyn,r}}$	Dynamic Young's modulus (resonance method)
$E_{\mathrm{dyn,u}}$	Dynamic Young's modulus (ultrasound method)
f_{b}	Bending strength
f_{c}	Compressive strength
λ	Thermal conductivity coefficient

1. Introduction

Material consumption increased by a factor of 10 in the 20$^{\mathrm{th}}$ century century (Krausmann et al., 2009) and the projected demand for materials is expected to at least double the levels of consumption from the beginning of the 21st century by 2050 (Allwood et al., 2011). As a response, the European Union attempted to initiate a transformation of linear models into circular economy (Huysman et al., 2017; COM, 2014; Commission et al., 2015) by introducing the initiative on A Resource-Efficient Europe (COM, 2011). This initiative proposes a strategy to involve all key stakeholders to achieve, in addition to other ambitious goals, high material efficiency in the construction sector and most of the construction and demolition waste (CDW) to be recycled by 2030. However, the implementation of the circular economy in this sector is hampered by weak legislation (Mittal and Sangwan, 2014a,b), low management commitment, and also by lack of adequate technologies or customer distrust (Esa et al., 2016; Mangla et al., 2017).

In this regard, concrete has the greatest potential to increase the sustainability of the construction sector. The worldwide use of concrete is more than double the use of other construction materials combined (Van Damme, 2018) and its production is associated with approximately 10% of global anthropogenic CO_2 emissions (Paris et al., 2016; da Silva and de Oliveira Andrade, 2017). Despite the negative impacts on concrete quality (Grabois et al., 2017), higher demands for mixing water (Bravo et al., 2018; Özalp et al., 2016), and technological challenges, supplementing natural quarried aggregates with recycled aggregates (Akhtar and Sarmah, 2018; Colangelo et al., 2018; Martínez et al., 2018; Xiao, 2018) or sand (Ding et al., 2020; Zou et al., 2021) has become a common practice for economic and environmental benefits (Ding et al., 2016; Pacheco-Torgal, 2020). However, this effort to replace quarried aggregates does not contribute to reductions in portland cement (PC) production, which is responsible for the massive carbon footprint (US Geological Survey & Orienteering S and US Geological Survey, 2009; Paris et al., 2016; da Silva and de Oliveira Andrade, 2017; Lee et al., 2018).

PC consumption has increased by almost 3,400% over the past 65 years (Scrivener et al., 2018) despite efforts to partially replace PC with various supplementary cementitious materials (SCMs), such as fly ash, different slags, microsilica, or metakaolin (Turner and Collins, 2013; Gao et al., 2015; Shojaei et al., 2015; Gholampour and Ozbakkaloglu, 2017; Nežerka et al., 2019). Many of these SCMs are produced by very pollutant and gradually disappearing industries (e.g., coal power plants, steel factories burning coke, etc.). Although the use of SCMs in the form of industrial by-products increases sustainability, it does not contribute to circularity (Marsh et al., 2022). To achieve both, it is desirable to efficiently replace PC with stripped paste generated during the crushing and disintegration of the waste concrete. However, the use of these recycled concrete fines (RCF), which represent approximately 40% of the weight of crushed concrete waste (Villagrán-Zaccardi et al., 2022), is disapproved or even forbidden by building codes due to commonly accepted misconceptions about their impact on concrete performance (Evangelista and de Brito, 2013), although efficient ways to increase reactivity and incorporate RCF into cementitious mixes have been found. The first way, although energetically demanding, is to exploit heat to increase the reactivity of RCF (Shui et al., 2008; Serpell and Lopez, 2013; Florea et al., 2014; Gastaldi et al., 2015; Lotfi and Rem, 2017). Alternatively, RCF can be ground (micronized) to distort the tetrahedral structure of α-SiO_2 and transform it into an amorphous form (Liu et al., 2014) and expose unhydrated cement particles (Prošek et al., 2020b). The reactivity of these disintegrated RCFs can be further enhanced with alkali additives, such as slag or fly ash (Prošek et al., 2019). Eventually, chemical compounds such as tannic acid (Wang et al., 2022), can also improve the binding of RCF to hydration products and improve the strength and durability of the cementitious material produced.

The goal of this study is to propose a technique for producing lightweight masonry blocks containing large amounts of micronized RCF without the need for significant technological changes in standard manufacturing processes or sacrifice in the performance of the end product. A well-documented design procedure based on our previous research (Prošek et al., 2019, 2020b; Nežerka et al., 2020) and the findings of other authors (Khatib, 2005; López-Uceda et al., 2016; González et al., 2021), comprehensive testing, and detailed life cycle assessment (LCA) (Pešta et al., 2020) are expected to contribute to gaining the trust of all involved parties, from investors and producers to environmental protection agencies. Standardized LCA procedures (Finkbeiner et al., 2006) were used not only to evaluate the elementary flows of materials and energies, but also to describe their potential secondary environmental impacts (Knoeri et al., 2013). The standardized LCA procedures involve a thorough inventory of energy and material consumption, as well as emissions associated with the production and use of a specific product or service to provide its overall environmental profile. It has been widely used in construction industry for optimization of a specific material/component, such as PC (Hossain et al., 2017), or composites, such as concrete (Turk et al., 2015; Vieira et al., 2016; Kleijer et al., 2017). It must be kept in mind that technical parameters of compared product have to be also considered, since materials with a smaller ecological footprint may have low strength resulting in the need to use higher amount of this material to provide the required load-bearing capacity (Marinković et al., 2017). In this study, the performance and all environmental impacts associated with the production of the developed lightweight masonry blocks were compared with the environmental product declaration and technical sheet of widely used aerated autoclaved concrete (AAC) blocks having similar technical parameters and use.

2. Materials

The extensive experimental program focused on the testing and design of cement-based foam material used for the production of lightweight masonry blocks. This composite material was produced using the following ingredients: (i) PC of a class CEM I/42.5R (EN 197-1:2011 (European Committee for Standardization, 2011)), (ii) RCF prepared by crushing and grinding 100-year-old concrete from monolithic columns used in interior using a high-energy electric mill (SBD 800 assembled by the Lavaris company, Czech Republic), (iii) microfibers (MFs) made of 100% recycled polypropylene produced for mortar/concrete reinforcement produced by the Trevos Košťálov company from the Czech Republic (having 32 µm in diameter and length of 4 mm), (iv) polycarboxylate-based/modified polycarboxylate-based superplasticizers (SPs) developed for ready-mix concrete (Table 1), dosed according to the recommendations by the manufacturers, (v) a foaming agent (FA) based on amides and sulfonic acid, and (vi) tap water. PC and RCF used in this study were characterized in detail by Prošek et al. (2020b), who dealt with recovery of anhydrous clinker and used the same input materials for experimental testing.

The amount of mixing water was reduced using SPs to support the FA responsible for the porous structure of the hardened material. FA was used in a 50% concentration to reach foamability of 35 ml/g and foam stability of 465 minutes. MFs were used to reinforce the brittle structure of the hardened composites. According to the technical sheets of the producer, the MFs had a density of 910 kg/m^3, exhibited the average tensile strength of $\geq$3.0 cN/dtex ($\sim$272 MPa), average elongation

Table 1: Summary of SPs used in this study.

	Name (brand)	Dosage [wt.%]	pH	Chloride content [%]	Dry extract [%]	Density [kg/dm^3]	Alkali content (Na_2O equiv.) [%]
SP1	Fortesil (Stachema)	0.8	9.75	<0.1	30.0	1.17	8.0
SP2	Premia 196 (Chryso)	0.8	7.50	<0.1	25.3	1.06	1.5
SP3	Premia 330 (Chryso)	1.0	6.50	<0.1	23.6	1.05	2.0
SP4	ViscoCrete-20 Gold (Sika)	2.5	4.50	<0.1	29.0	1.05	1.0

at rupture ≥50%, and the elastic stiffness of ∼4 GPa. The surface of the MFs was smooth since the filaments were manufactured using the standard technology of melt spinning. The amount of MFs was determined based on our preliminary studies, supported by the findings of Raj et al. (2020).

The chemical composition of PC and RCF used in this study was determined using X-ray fluorescence spectroscopy (XRF) according to the EN 196-2:2013 (European Committee for Standardization, 2013). XRF analysis was performed using a Spectro Xepos spectrometer equipped with 50 W/60 kV X-ray emitters. The list of detected oxides is presented in Table 2; equivalent concentrations of clinker phases were calculated based on these values using the Bogue formula, defined in the ASTM C114 standard (ASTM C114, 2018).

PC used in this study was rich in C_3S (74.6%) and contained smaller proportions of C_3A (8.1%) and C_2S (7.2%). Such an allitic PC was supposed to exhibit an early strength gain. The analyzed RCF powder contained high amounts of SiO_2 due to the presence of ground siliceous sand of 0–1 mm fraction, present in the disintegrated concrete. The high amounts of CaO and loss on ignition (LOI) in RCF can be attributed to the high content of the hydrated cementitious matrix.

Table 2: Concentration of the most important oxides and LOI [%] identified using XRF for PC and RCF used in this study.

	CaO	SiO_2	Fe_2O_3	Na_2O	MgO	Al_2O_3	SO_3	LOI	Other
PC	64.8	20.1	2.51	0.13	1.92	4.02	3.01	3.05	0.45
RCF	23.8	36.4	3.13	1.36	1.43	7.56	1.58	22.7	2.04

The particle size distribution curves for both PC and RCF, determined using a Fritsch Analyssete 22 MicroTec Plus laser diffraction particle size analyzer, are provided in Figure 1. RCF contained finer particles than PC; the fineness of PC and FRC corresponds to their specific surface, determined using the Blaine method (Matest E009 device), equal to 380, and 860 m^2/kg, respectively.

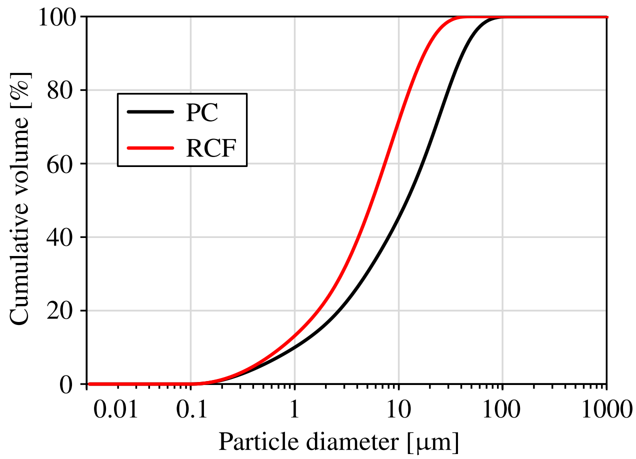

Figure 1: Particle size distribution curves for PC and RCF.

2.1. *Tested mixtures*

The mixture optimization procedure consisted of three stages during which different mixtures were prepared and tested (Tables 3–5). For the first two optimization stages, the water-to-cement ratio (w/c) was adjusted so that the flow test result (FTR) reached 180±5 mm after 15 blows. The optimum w/c, strongly influenced by the presence of fine RCF particles, was then used for the final set tested within Stage 3. The flow test was performed according to EN 12350-2 (European Standard EN 12350-5, 2009). During all stages, fresh pastes were placed in molds, compacted using a shaking table, and removed from molds after 24 h. Hardening took place in a laboratory at 22±1 °C and relative humidity of 50±6% for 28 days. The bulk density (ρ_{b}) was determined according to the EN 12390-7 standard (EN-, 2009) by employing the gravimetric method.

2.1.1. *Mixtures for Stage 1*

The first set of mixtures (Table 3) consisted of hardened pastes and was used to determine the appropriate PC-to-RCF ratio. The effort was to maximize the RCF content while having the hardened paste compact without disintegration during manipulation with the specimens or low-intensity loading. The FTRs of these mixtures indicate poorer workability of pastes containing RCF as a result of adhesion of this fine-grained component having a large specific surface. This effect is not in accordance with the requirements on sustainable materials and therefore the large water demands had to be reduced using suitable SPs, selected in Stage 2.

Table 3: Composition of mixtures for RCF content optimization, FTR and bulk densities of hardened mortars (Stage 1).

Mix	PC	RCF	w/c	ρ_b	FTR
	[wt.%]			[kg/m^3]	[mm]
10/0	100	0	0.35	2298±16	179
9/1	90	10	0.40	2023±15	180
8/2	80	20	0.46	1970±20	179
7/3	70	30	0.56	1957±7	176
6/4	60	40	0.67	1862±10	177
5/5	50	50	0.84	1837±9	177
4/6	40	60	1.08	1810±11	178
3/7	30	70	1.50	1795±6	180
2/8	20	80	2.35	1790±5	181
1/9	10	90	4.90	1785±8	180

2.1.2. *Mixtures for Stage 2*

The second set (Table 4) consisted of mixtures that have the optimal PC-to-RCF ratio (40:60; see Section 4.1) and different SPs. In Stage 2, a suitable SP providing the most compact matrix at the micro-scale, thus exhibiting a superior strength and stiffness, was selected. w/c varied due to the different amounts and efficiency of the SPs used in the study.

2.1.3. *Mixtures for Stage 3*

The third set of samples (Table 5) was lightened with FA and reinforced with MFs. The objective of the Stage 3 testing was to determine whether it is favorable to add MFs and select an

Table 4: Composition of mixtures for testing the effects of different SPs (Stage 2).

Mixture	PC	RCF	SP1	SP2	SP3	SP4	w/c	ρ_b	FTR
	[wt.%]		[wt.% of PC]					[kg/m^3]	[mm]
4/6 SP1	40	60	0.8	–	–	–	0.93	1845±16	175
4/6 SP2	40	60	–	0.8	–	–	0.93	1852±13	175
4/6 SP3	40	60	–	–	1.0	–	0.93	1913±19	180
4/6 SP4	40	60	–	–	–	2.5	0.80	1993±15	178

appropriate amount of FA to obtain blocks exhibiting sufficient strength while maintaining low heat conductivity. FTR for this set was not measured because the mixtures were liquid before foaming.

Table 5: Composition of mixtures for testing the effects of FA and MFs (Stage 3).

Mixture	PC	RCF	SP4	FA	MFs	w/c	ρ_b
	[wt.%]		[wt.% of PC]				[kg/m^3]
4/6 SP4 A	40	60	2.5	3.00	2.5	0.50	810±5
4/6 SP4 B	40	60	2.5	2.25	2.5	0.50	801±4
4/6 SP4 C	40	60	2.5	2.25	–	0.50	980±10
4/6 SP4 D	40	60	2.5	1.50	2.5	0.50	1110±11

3. Methods

Standardized test methods for macroscopic samples, commonly adopted in both industry and research, were used to evaluate the key parameters of the developed composites. All tests were performed on 28 days old specimens at 22±1 °C and relative humidity of 50±5% (CEN, accessed November 19, 2021).

3.1. *Stiffness assessment*

Impact resonant frequency testing according to the ASTM C215 Standard (AST, 2014) was measured for six 40×40×160 mm specimens representing each mixture using the Brüel & Kjaer

3560-B-120 device. The dynamic Young's modulus was determined from the frequency response function according to the formula presented in the ASTM C215-14 Standard:

$$E_{\mathrm{dyn,r}} = \frac{4Lmf_{\mathrm{I}}^2}{bt}, \tag{1}$$

where L, b, and t are the length, width, and thickness of a specimen, respectively, m is its mass, f_{I} is the measured fundamental longitudinal resonant frequency.

Furthermore, the stiffness of the specimens was evaluated based on the velocity of ultrasound pulse wave propagation, v_{u}, according to the ASTM E1876-01 Standard (AST, 2006), using the Pundit Lab device equipped with 54 kHz probes attached to the surface of the specimens using sonogel. The dynamic Young's modulus was determined on the basis of v_{u} as

$$E_{\mathrm{dyn,u}} = \frac{\rho_{\mathrm{b}} v_{\mathrm{u}}^2 (1+\nu)(1-2\nu)}{1-\nu}, \tag{2}$$

where ν is its Poisson's ratio.

3.2. *Determination of strength*

Destructive tests were carried out using a Heckert FP100 loading frame with displacement-controlled loading at the rate of 0.1 mm/min. The bending strength was determined based on the load-displacement records from three-point bending tests performed using the 40×40×1600 mm prismatic specimens as for the stiffness testing according to

$$f_{\mathrm{b}} = \frac{3F_{\mathrm{b,max}} L_{\mathrm{s}}}{2b^2 t}, \tag{3}$$

where $F_{\mathrm{b,max}}$ is the maximum force reached during the bending test and L_{s} is the span between the supports, here equal to 100 mm, b is the cross-section height, and t is the cross-section width.

Uniaxial compression tests were carried out on 40×40×40 mm cubic specimens extracted from the halves of specimens broken during the bending test; each mixture was represented by twelve specimens. The compressive strength was calculated from the maximum force reached during the test, $F_{\mathrm{c,max}}$, as

$$f_{\mathrm{c}} = \frac{F_{\mathrm{c,max}}}{bt}, \tag{4}$$

where $F_{\mathrm{c,max}}$ is the maximum force reached during the compression test.

3.3. Evaluation of heat transfer properties

The thermal conductivity coefficient λ was evaluated for 150×150×150 mm specimens using an ISOMET 2104 (Applied Precision) heat transfer analyzer, equipped with API210411 and API210403 surface probes capable of measurements in the ranges of 0.04–0.3 W/mK and 0.3–2.0 W/mK, respectively, and with the accuracy of ±5 %. The device employs the dynamic method based on monitoring the response of an examined material to heat flow impulses. Each mixture was represented by six specimens, each measured three times in a different orientation and position of probes.

A scheme of the three-stage optimization process involving all the methods used to evaluate the performance of the developed composites and number of specimens for each test are presented in Figure 2.

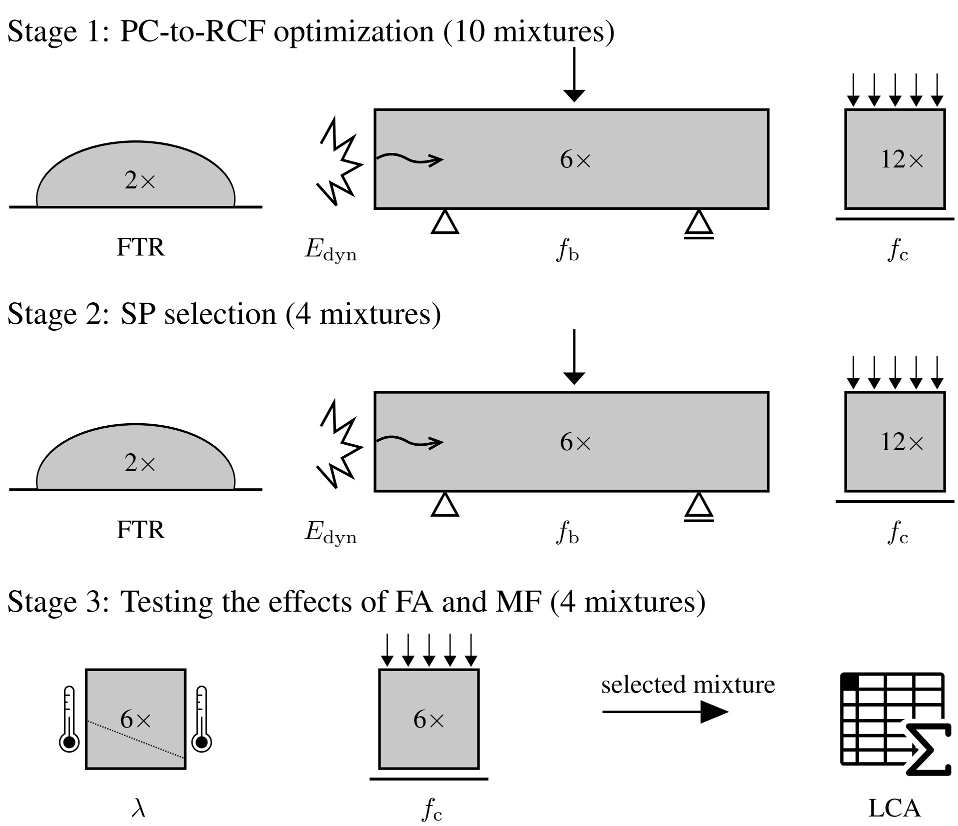

Figure 2: Three-stage experimentally-based development of a lightweight cementitious composite material containing RCF; number of tested specimens, experimental methods, and output parameters used for performance assessments.

3.4. LCA

LCA, standardized by ISO 14040 (Finkbeiner et al., 2006) was performed according to procedures for building products provided in the EN 15 804+A2 standard (CEN, accessed November 27, 2020). The environmental impacts of one ton of the developed blocks containing RCF were assessed to evaluate its environmental burdens and benefits. The system boundaries included the following lifecycle phases: extraction of raw material, production of materials (including RCF), transport, preparation of the concrete mixture, and the end-of-life product phase. The end-of-life phase involved deconstruction, CDW transport, and landfilling (Figure 3). The use phase for the developed block was not considered, and the reference service life was assumed to exceed 50 years.

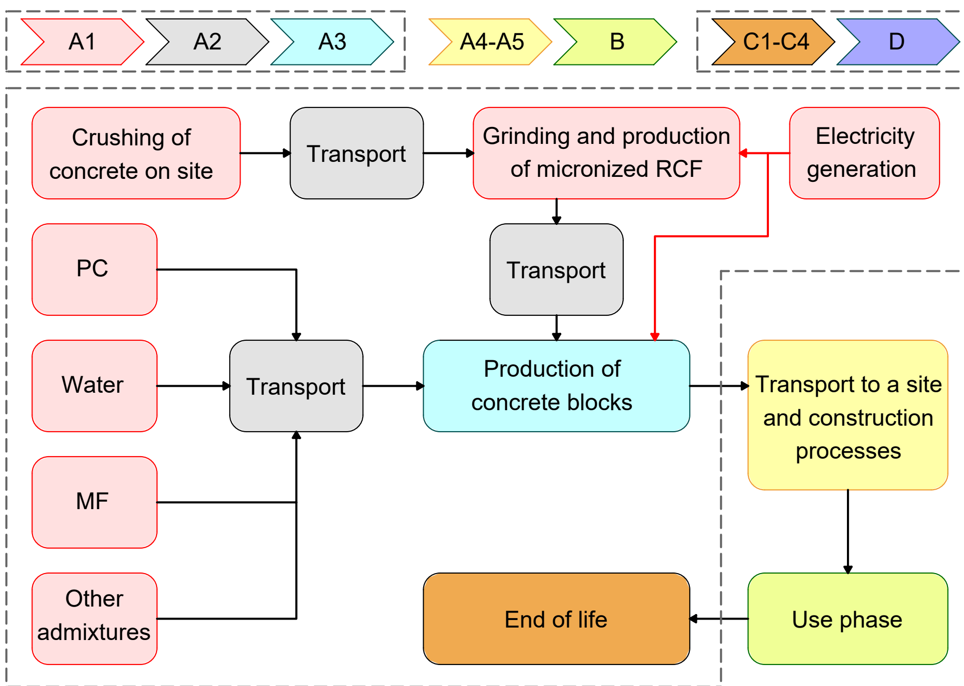

Figure 3: Processes involved in the modeled system boundaries (separated with the dashed lines) for the developed block production; life-cycle phases according to EN 15 804+A2 (CEN, accessed November 27, 2020): A1 = raw material extraction and supply (light red), A2 = transport (grey), A3 = manufacturing (light blue), A4–A5 = construction (yellow), B1–B7 = the use phase (green), C1–C4 = end-of-life phase (orange), D = benefits and loads beyond the system boundary (blue, not considered in our study).

A Gabi Professional software (Gabi Software, accessed October 30, 2020) was used to model all the considered system boundaries and describe elementary energies and material flows. Next,

Table 6: Specific distances for the modeled transport of materials, based on real distances between the involved suppliers and facilities near Prague, Czech Republic; pipeline transport of water has been neglected.

Material transported	Distance [km]
PC	70
Recycled concrete	70
RCF	52
Chromium milling parts	100
FA	200
MFs	280
SP	200
CDW collection (used blocks)	100 (assumed)

the potential impacts caused by these flows were assessed. Generic data was used for models of nonspecific processes such as transport, production of electricity mix (for the Czech Republic), CDW landfilling, and petroleum supply (Kupfer et al., 2020). Generic data from the Gabi database were used for ingredients except for RCF, for which input and output had to be calculated. These calculations were based on data provided by producers of recycled aggregate who prepared RCF from the 0/4 concrete waste fraction using a high-speed mill; the data collected during the processing of RCF were: Electricity consumption equal to 6.25 kWh/t and wearing of the mill at a rate of 268 g/t. Transport was modeled considering a generic process for a truck of the Euro 5 emission category with a specific distance provided in Table 6.

4. Results and discussion

4.1. RCF content optimization

Finding the optimal PC-to-RCF ratio to ensure sufficient matrix strength (set in advance to $f_c \geq 50$ MPa and $f_b \geq 4$ MPa, based on experience (Topič et al., 2017, 2018) to sustain common manipulation without disintegration), while keeping the RCF content as high as possible was a crucial part of the optimization procedure. Stiffness of specimens was not considered crucial for the selecting the most suitable mixture, however, keeping $E_{dyn} \geq 15$ GPa was expected. The difference between Young's moduli $E_{\mathrm{dyn,r}}$ and $E_{\mathrm{dyn,u}}$ (Figure 4) for less than 40 wt.% of RCF indicates a low degree of homogeneity due to the presence of cracks or large voids (Brožovský and Dufka, 2015), common for cementitious pastes lacking stiff inclusions (Nežerka et al., 2017). Shrinkage-induced micro-cracks (Nežerka et al., 2020) present in pastes lacking reinforcement provided by the RCF inclusions have large impact on natural frequencies measured to evaluate $E_{\mathrm{dyn,r}}$. The presence of these micro-cracks and the fact that RCF acts as a micro-filler is responsible for non-linearity in the measured E_{dyn} (Niewiadomski et al., 2021).

The addition of RCF resulted in a linear decrease in f_{c}, while f_{b} peaks at the 40:60 PC-to-RCF ratio (60 wt.% of RCF), selected for further optimization as optimum. The development of f_{c} roughly correlates with ρ_{b} (Table 3) and therefore also with porosity, which is consistent with the findings of other authors dealing with the incorporation of RCF into cementitious composites (Ma and Wang, 2013; Bordy et al., 2017; Quan and Kasami, 2018). This conjecture is also supported by the linear decrease in $E_{\mathrm{dyn,u}}$ with the replacement of PC with RCF. The peak in f_{b} can be attributed to the reinforcing effect provided by RCF, which plays the role of fine aggregate that increases fracture toughness (Strange and Bryant, 1979; Nežerka et al., 2014, 2017), prevents shrinkage-induced cracks to develop and propagate (Nežerka et al., 2020), and impedes opening and propagation of micro-cracks due to tensile stresses (Strange and Bryant, 1979; Karihaloo et al., 1993; Rhee et al., 2019). Similar results have been obtained by Prošek et al. (2020a) when studying the effects of limestone powder in cementitous pastes. The drop in f_{b} beyond the 40:60 threshold is attributed to a lack of binder (PC).

4.2. SP selection

Reducing the amount of water was another crucial step in optimizing the mixture, as large amounts negatively affect the stability of the foam after the addition of FA (Raj et al., 2019). Setting general rules for the selection of SPs is difficult as their performance depends on the type of cement and aggregates used. Here, the selection was based on the impact of individual SPs on the mechanical properties of hardened mortars. These properties are influenced by both the porosity and the uniformity of the dispersion of the cement grains, as suggested by Carazeanu (2002).

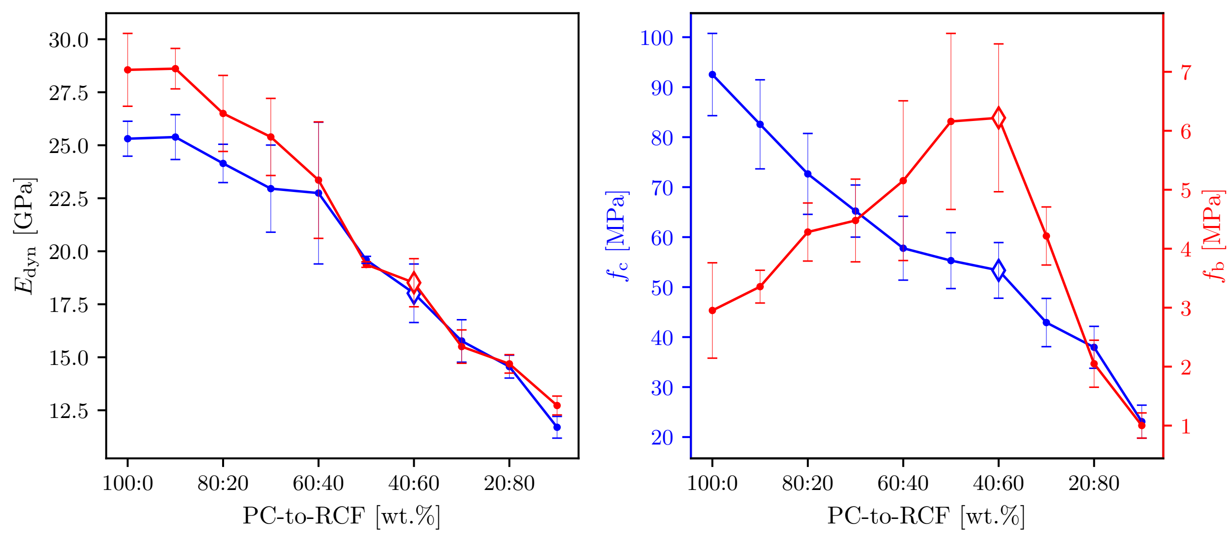

Figure 4: Relationship between the PC-to-RCF ratio and mechanical properties of hardened cementitious pastes (Stage 1 testing); the mixture selected for further development stages (40:60) is highlighted with diamond markers.

The impact of SPs on the porosity of mortars correlates with the values of ρ_{b}, provided in Table 4. In this regard, the use of SP4 resulted in the most compact matrix, reflected also by the highest values of E_{dyn} and f_{c} (Figure 5), which is consistent with the findings by Quan and Kasami (2018) and Barbudo et al. (2013). All mortars tested within Stage 2 exhibited a brittle behavior and large scatter in the measured f_{b} and therefore high standard deviations. For this reason, MFs were added to the 4/6 SP4 mixture in Stage 3 of the development.

4.3. FA and MFs content optimization

The results of testing at Stage 3 clearly indicate the importance of MFs and the effects of FA on the mixture. The mixtures 4/6 SP4 B and 4/6 SP4 C were identical, except for the content of MFs. The 4/6 SP4 C mixture without MFs exhibited, despite the lower ρ_{b} (Table 5), 28% lower f_{c} and 138% higher λ (Figure 6). This indicates both the reinforcing effect of MFs as well as their positive impacts on the pore size distribution, which has also been suggested in the studies by Namsone et al. (2017) and Steshenko et al. (2017). The measured values of λ correspond to the results of the study by Ganesan et al. (2015) who reported for aerated concrete a linear relationship

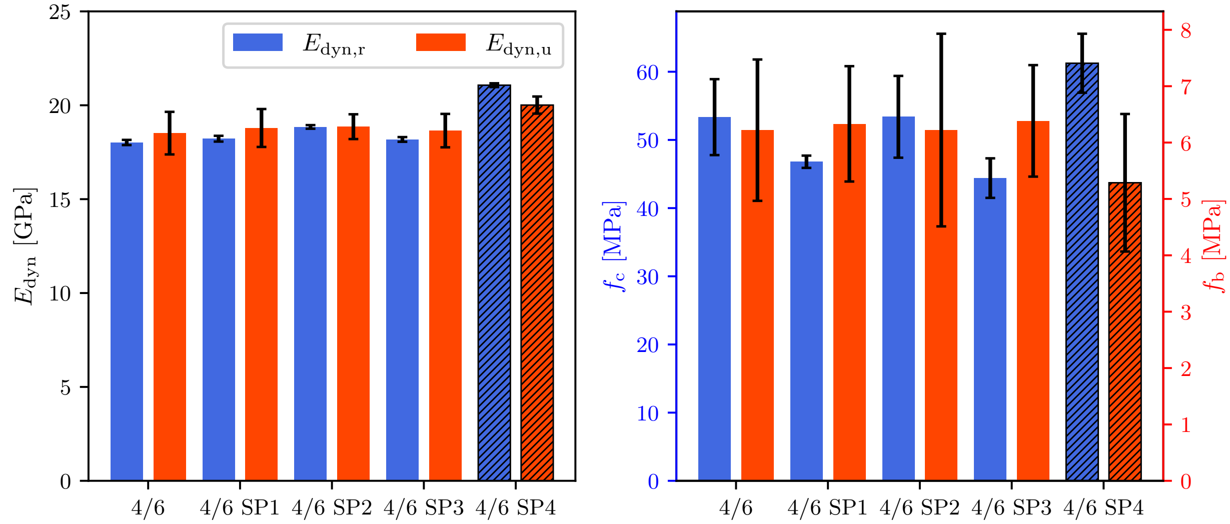

Figure 5: Effect of different SPs on mechanical properties of hardened cementitious pastes (Stage 2 testing); the mixture selected for further development stage (4/6 SP4) is highlighted with a hatch.

between λ (range 0.24–0.74 W/mK) and ρ_b (range 700–1400 kg/m^3) .

Taking thermal conductivity as the key parameter, mixture 4/6 SP4 B was selected for large-scale production and assessment of environmental impacts. The blocks made of this mixture exhibited low heat conductivity, $\lambda = 0.21 \pm 0.02$ W/mK, while having sufficient compressive strength, $f_c = 7.1 \pm 0.5$ MPa. This strength exceeds the lower limit set in advance to 5 MPa.

4.4. Large-scale production

To verify applicability of the 4/6 SP4 B, the mixture preparation procedure was translated into semi-production in a concrete plant. The procedure encompassed a whole industrial mixture preparation procedure: mixture preparation, its transport, and placement in molds. The mixture preparation was carried out using a planetary mixer with a whirling drum at the Destro company located in Kladno near Prague, Czech Republic. First, all ingredients were mixed, followed by the addition of water with SP4. FA was aerated using an industrial foam generator and the foam was mixed with fresh mortar and the final mixture was then transported to the molding site using an automatic concrete mixer. Here, the mixture was placed in two molds, each for 44 blocks with

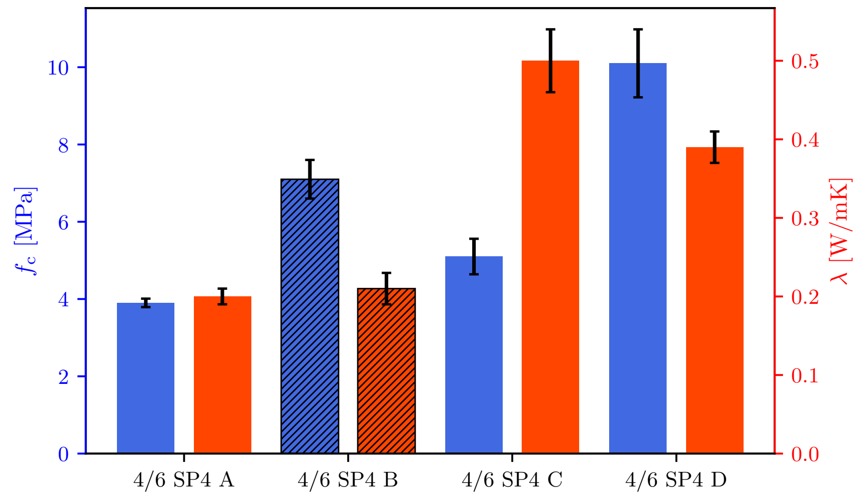

Figure 6: Effect of FA and MFs on mechanical properties of hardened aerated cementitious composites (Stage 3 testing); the mixture selected for large-scale production and LCA (4/6 SP4 B) is highlighted with a hatch.

dimensions of 500×250×175 mm (Figure 7).

Although this was the first semi-production run, the resulting product had properties comparable to those of common commercially produced foam silicates. A 10 m^2 external wall (Figure 8) was constructed from lightweight hardened blocks in the premises of the University Center for Energy Efficient Buildings of the Czech Technical University in Prague and was exposed to the outdoor environment. The wall is currently subject to long-term monitoring of the moisture content, thermal conductivity, and structural properties during real operating conditions.

4.5. Environmental impacts

From the assessment of environmental impacts (Tables 7 and 8) it is clear that the production of raw materials needed to manufacture the developed lightweight masonry blocks contributes the most to almost every indicator. This is most significant for indicators related to CO_2 production, resource use, eutrophication, energy demands, waste disposal, and toxicity and radioactivity. On the other hand, indicators related to water use are positively influenced by the exploitation of recycled materials. The revised version of EN 15 804+A2 standard (CEN, accessed November 27, 2020) includes calculations for end-of-life benefits in Annex D and these end-of-life benefits reflect circularity and recycling and result in a negative value for the Water use and Use of net

Figure 7: Pouring of the industrially produced mixture (4/6 SP4 B) into large-scale molds.

Figure 8: Masonry wall assembled from industrially produced lightweight blocks for long-term monitoring of thermal and hygric properties.

fresh water indicators. Indirectly, concrete production contributes almost 20% to the impact in the Ionising radiation category, being the result of the production of electricity for the processes. The production phase and transport processes are responsible for negligible impacts compared to the production of raw materials.

4.5.1. Contribution analysis

All processes were evaluated to determine their contributions to the potential environmental impact per life cycle of 1 t of the lightweight blocks made of the 4/6 SP4 B mixture. All significant contributions (>10% of the total impact) are listed in Table 9 and graphically represented in Figure 9.

Concrete recycling contributes beneficially to several impact categories and significantly mitigates the overall use of resources (mineral and metals). Replacement of PC with RCF directly reduces PC production, having the greatest impact on climate change to which it contributes by more than 80%. At the same time, PC production significantly impacts Acidification, Photochemical ozone creation, Resource use (fossil), and Water use categories. These categories are also greatly affected by the contribution of the landfilling process. SP production (used in the amount of 10 kg/1 t of the lightweight blocks) contributes by 96% to ozone depletion and increases the results for other impact indicators, including Eutrophication freshwater, Resource use (mineral and metals), and Water use, as well. In this regard, the use of more user-friendly solutions, such as ultrafine mineral admixtures (Han et al., 2022), should be considered.

These findings clearly justify the effort to incorporate RCF into PC-based composites. The results of a study on the potential environmental impacts of different PC-to-RCF ratios are provided in Table 10, which shows an almost perfectly linear relationship between the critical indicators and the PC-to-RCF ratio. This ratio could be further increased when using recycled cement having binding properties; the technology based on magnetic separation of stripped cement paste and its thermoactivation was proposed and scrutinized by Sousa and Bogas (2021); Sousa et al. (2022).

4.5.2. Comparison with AAC blocks

A scenario analysis was carried out to compare the environmental impacts of the developed lightweight blocks (4/6 SP4 B) with impacts of commercially produced AAC blocks (commercial

Table 7: Environmental indicators calculated for 1 t of the developed lightweight blocks (4/6 SP4 B) according to the EN 15 804+A2 standard (CEN, accessed November 27, 2020), part 1.

Indicator	Total	Production of materials	Transport	Concrete production	End of life
Climate change, total [kg CO_2 eq.]	334	298	4.44	9.39	22.8
Climate change, fossil [kg CO_2 eq.]	334	297	4.45	9.33	23,3
Climate change, biogenic [kg CO_2 eq.]	455	58	-0.04	0.06	-0.5
Climate change, land use and land use change [kg CO_2 eq.]	0.312	0.196	0.03	0.001	0.084
Ozone depletion [kg CFC-11 eq.]	1.79×10^{-6}	1.79×10^{-6}	4.38×10^{-13}	7.05×10^{-11}	3.63×10^{-11}
Acidification [Mole of H^+ eq.]	0.70	0.51	0.15	0.22	0.15
Eutrophication, freshwater [kg P eq.]	3.71×10^{-3}	3.61×10^{-3}	1.59×10^{-5}	2.36×10^{-5}	5.55×10^{-5}
Eutrophication, marine [kg N eq.]	0.19	0.13	6.81×10^{-3}	4.26×10^{-3}	0.05
Eutrophication, terrestrial [Mole of N eq.]	2.09	1.42	0.08	0.04	0.55
Photochem. ozone formation, human health [kg NMVOC eq.]	0.57	0.42	0.01	0.01	0.13
Resource use, minerals and metals [kg Sb eq.]	2.31×10^{-4}	2.27×10^{-4}	4.49×10^{-7}	1.05×10^{-6}	2.39×10^{-6}
Resource use, fossils [MJ]	2090	1580	58.5	144	306
Water use [m^3 world equiv.]	-20.3	-22.2	0.05	0.13	1.72

Table 8: Environmental indicators calculated for 1 t of the developed lightweight blocks (4/6 SP4 B) according to the EN 15 804+A2 standard (CEN, accessed November 27, 2020), part 2.

Indicator	Total	Production of materials	Transport	Concrete production	End of life
Use of renewable primary energy (PERE) [MJ]	318	244	4.1	32.1	37.1
Total use of renewable primary energy resources (PERT) [MJ]	318	244	4.1	32.1	37.1
Use of non-renewable primary energy (PENRE) [MJ]	2090	1580	58.7	144	307
Total use of non-renewable primary energy resources (PENRT) [MJ]	2090	1580	58.7	144	307
Use of renewable secondary fuels (RSF) [MJ]	1.64×10^{-22}	1.64×10^{-22}	0.00	0.00	0.00
Use of non renewable secondary fuels (NRSF) [MJ]	1.93×10^{-21}	1.93×10^{-21}	0.00	0.00	0.00
Use of net fresh water (FW) [m^3]	-7.09×10^{-2}	-1.80×10^{-1}	4.68×10^{-3}	4.64×10^{-2}	5.85×10^{-2}
Hazardous waste disposed (HWD) [kg]	8.40×10^{-4}	8.40×10^{-4}	3.11×10^{-10}	6.82×10^{-9}	1.07×10^{-8}
Non-hazardous waste disposed (NHWD) [kg]	1000	3.02	0.01	0.06	1000
Radioactive waste disposed (RWD) [kg]	6.63×10^{-2}	4.42×10^{-2}	1.09×10^{-4}	1.96×10^{-2}	2.35×10^{-3}
Particulate matter [Disease incidences]	8.37×10^{-6}	6.61×10^{-6}	8.68×10^{-8}	1.65×10^{-7}	1.51×10^{-6}
Ionising radiation, human health [kBq U235 eq.]	7.61	6.03	0.02	1.30	0.26
Ecotoxicity, freshwater [CTUe]	1070	785	41.5	53.5	188
Human toxicity, cancer [CTUh]	6.50×10^{-8}	4.47×10^{-8}	8.55×10^{-10}	1.06×10^{-9}	1.83×10^{-8}
Human toxicity, non-cancer [CTUh]	4.95×10^{-6}	2.88×10^{-6}	5.27×10^{-8}	7.35×10^{-8}	1.94×10^{-6}
Land Use [Pt]	466	306	24.8	45.9	89.4

Table 9: Relative contributions [%] of processes (listed only those contributing by more than 10% of the total impact in a category)

Indicator	Concrete recycling	Electricity generation	PC production	Landfilling	MFs production	Recycling plant maintenance	SP production
Climate change, total [kg CO_2 eq.]	-2.87	2.81	81.44	4.34	5.06	0.31	3.32
Ozone depletion [kg CFC-11 eq.]	0.00	0.00	0.00	0.00	0.01	3.01	96.04
Acidification [Mole of H^+ eq.]	-1.30	3.10	61.77	15.12	3.14	0.77	5.55
Eutrophication, freshwater [kg P eq.]	0.16	0.64	3.42	0.68	0.85	11.81	80.30
Photochemical ozone formation, human health [kg NMVOC eq.]	-0.42	2.07	60.81	14.45	4.50	0.53	4.89
Resource use, mineral and metals [kg Sb eq.]	-12.73	0.45	7.84	0.67	1.72	10.08	91.23
Resource use, fossils [MJ]	-4.08	6.89	34.31	9.33	27.99	0.67	11.41
Water use [m^3 world equiv.]	-160.59	0.65	13.55	8.03	1.85	2.44	27.88
Particulate matter [Disease incidences]	-3.18	1.97	71.45	15.53	4.16	0.73	3.85
Ionising radiation, human health [kBq U235 eq.]	3.02	17.08	45.60	3.06	6.81	2.09	13.66
Ecotoxicity, freshwater [CTUe]	1.40	5.00	22.15	10.19	25.98	3.15	16.65
Human toxicity, cancer [CTUh]	-9.28	1.63	28.31	25.69	10.77	19.48	17.66
Human toxicity, non-cancer [CTUh]	-2.33	1.49	49.95	37.40	6.81	0.40	2.14
Land Use [Pt]	3.27	9.87	41.78	9.13	6.87	1.75	6.47

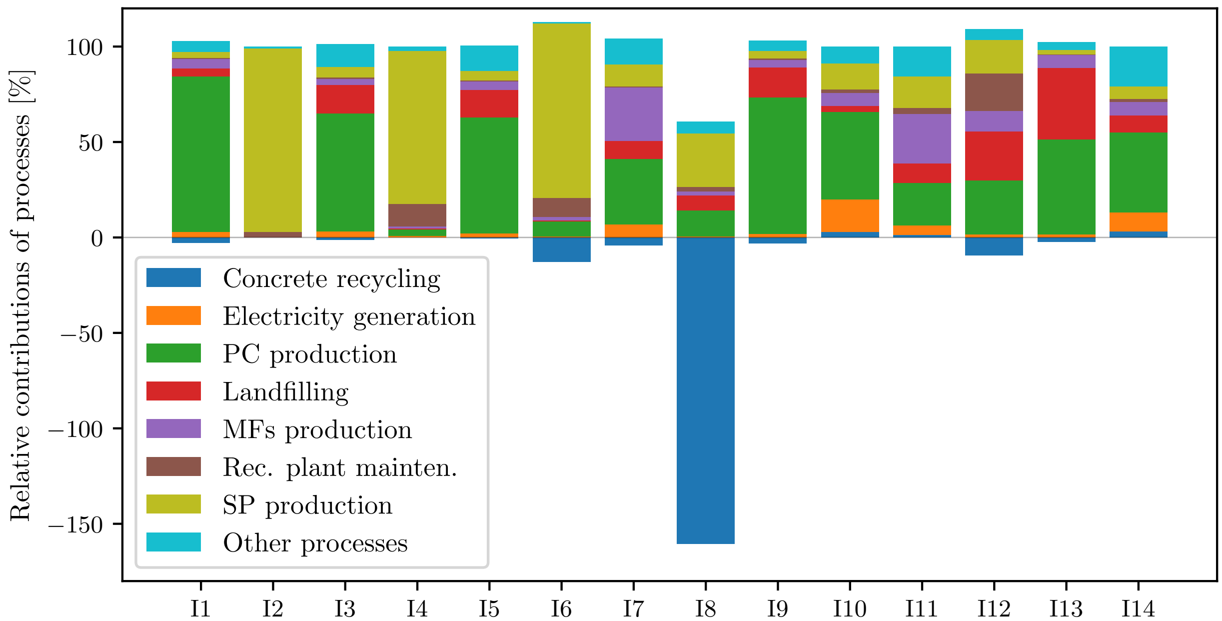

Figure 9: Graphical representation of results provided in Table 9 to show relative contributions [%] of crucial processes to selected indicators: I1 = Climate change, total; I2 = Ozone depletion; I3 = Acidification; I4 = Eutrophication, freshwater; I5 = Photochem. ozone formation, h. health; I6 = Resource use, mineral and metals; I7 = Resource use, fossils; I8 = Water use; I9 = Particulate matter; I10 = Ionising radiation, h. health; I11 = Ecotoxicity, freshwater; I12 = Human toxicity, cancer, I13 = Human toxicity, non-cancer, I14 = Land use.

Table 10: Selected environmental indicators calculated for 1 t of the developed lightweight blocks (4/6 SP4 B) according to the EN 15 804+A2 standard (CEN, accessed November 27, 2020), considering various PC/RCF ratios.

Indicator	55/45	50/50	45/55	**40/60**	35/65	30/70	25/75
Climate change, total [kg CO_2 eq.]	435	400	366	334	298	264	230
Ozone depletion [kg CFC-11 eq.]	1.78×10^{-6}	1.78×10^{-6}	1.78×10^{-6}	1.79×10^{-6}	1.79×10^{-6}	1.80×10^{-6}	1.80×10^{-6}
Acidification [Mole of H^+ eq.]	0.86	0.80	0.75	0.70	0.64	0.59	0.54
Eutrophication, freshwater [kg P eq.]	3.64×10^{-3}	3.66×10^{-3}	3.69×10^{-3}	3.71×10^{-3}	3.73×10^{-3}	3.75×10^{-3}	3.78×10^{-3}
Eutrophication, marine [kg N eq.]	0.23	0.22	0.20	0.19	0.18	0.17	0.15
Eutrophication, terrestrial [Mole of N eq.]	2.50	2.36	2.22	2.09	1.94	1.80	1.67
Photochemical ozone formation, human health [kg NMVOC eq.]	0.69	0.65	0.61	0.57	0.52	0.48	0.44
Resource use, mineral and metals [kg Sb eq.]	2.39×10^{-4}	2.37×10^{-4}	2.34×10^{-4}	2.31×10^{-4}	2.28×10^{-4}	2.26×10^{-4}	2.23×10^{-4}
Resource use, fossils [MJ]	2360	2270	2170	2090	1990	1900	1810
Water use [m^3 world equiv.]	-11.4	-14.5	-17.5	-20.3	-23.6	-26.6	-29.6

name Sysmic Idro[1], manufactured by Gasbeton, Italy; $\rho_b = 580$ kg/m^3), having similar structural and thermal insulation properties (Gasbeton, accessed October 30, 2021) and the same intended use. These AAC blocks were also selected because according to the data in the Environdec database (Environdec, accessed October 30, 2021), the environmental impacts were assessed according to the same standard.

The results of the scenario analysis are provided in Table 11. In most categories, the developed lightweight block reached better results than the AAC block, except for the Climate change, which is by the biggest share impacted by the production of needed PC. However, the available LCA calculations for both masonry blocks were limited only to the cradle-to-gate scope, including only the A1-A3 phases and omitting the end-of-life phase. Furthermore, the developed blocks were heavier ($\rho_b = 580$ kg/m^3) and therefore 1 m^3 contained significantly higher amount of material and presumably exhibited higher strength (the manufacturer of AAC blocks declares a compressive strength of 5 MPa). Despite these facts, the difference in the impact on the Climate change category is rather marginal. Moreover, the end-of-life stage of RCF utilized for the production of the developed lightweight blocks presents a large environmental burden, which is mitigated by the utilization of RCF. It can be assumed that the recyclability and service life of both materials are very similar (Zou et al., 2022), but this hypothesis will be scrutinized in future studies.

5. Conclusion

This study provides compelling evidence on the need to reuse concrete structural elements to increase sustainability and circularity in the construction sector. The disintegration of concrete elements, the transport of materials and the use of the disintegrated material to partially replace portland cement (PC) and aggregates in the production of new products unequivocally contribute to the circularity and protection of natural resources, but the energy demands and carbon footprint associated with these processes are still significant.

In this study, the finest fraction of the discarded concrete was micronized and used as a supplementary material to replace PC in the production of lightweight masonry blocks. This fraction

[1]https://environdec.com/library/epd3048

Table 11: Comparison between the environmental performance (environmental impact indicators) of the developed lightweight blocks (4/6 SP4 B) containing RCF and commercially produced AAC blocks (results for critical impact parameters, related to 1 m^3); limited to phases A1–A3.

	4/6 SP4 B	AAC
Climate change, total [kg CO_2 eq.]	249	232
Ozone depletion [kg CFC-11 eq.]	1.43×10^{-6}	1.90×10^{-3}
Acidification [Mole of H^+ eq.]	0.44	0.63
Eutrophication, freshwater [kg P eq.]	2.92×10^{-3}	2.35×10^{-2}
Eutrophication, marine [kg N eq.]	0.11	0.36
Eutrophication, terrestrial [Mole of N eq.]	1.23	2.45
Photochemical ozone formation, human health [kg NMVOC eq.]	0.35	1.03
Resource use, mineral and metals [kg Sb eq.]	1.83×10^{-4}	2.69×10^{-3}
Resource use, fossils [MJ]	1430	1790
Water use [m^3 world equiv.]	-17.6	14.0

typically contains aggregate fragments and hardened cement paste and represents a huge environmental burden. The experimental agenda was aimed on thorough testing and optimization of mixtures to yield a product that is competitive with commercially produced lightweight blocks made of aerated autoclaved concrete (AAC). The optimized mixture selected for large-scale industrial production was based on the mixture of PC and recycled concrete fines (RCF) in a 2:3 wt.% ratio, respectively. Higher ratio of RCF resulted in a paste/matrix that exhibited inferior strength. The workability of the fresh mortar was adjusted using a superplasticizer (SP), and the aerated structure was formed using a foaming agent added to the fresh mortar during the mixing process. The porous structure was reinforced with recycled polypropylene microfibers, needed to ensure sufficient strength. The blocks made of the optimized mixture exhibited low heat conductivity, $\lambda = 0.21 \pm 0.02$ W/mK, and a compressive strength $f_\mathrm{c} = 7.1 \pm 0.5$ MPa. Eventually, the industrial large-scale production of the developed blocks was tested in a concrete production plant, which included all the preparation procedures for mixing and placement, proving feasibility of the proposed mixture for practical applications. Hardened blocks were used to build an external masonry wall, which is currently under long-term monitoring of its behavior.

The detailed knowledge of all the processes needed for the production of lightweight blocks containing a large amount of RCF allowed for a precise life-cycle assessment (LCA) and comparison with the environmental performance of common AAC blocks. The LCA results suggest that replacing PC with RCF leads to considerable savings in raw material production, thus significantly reducing CO_2 production, resource use, eutrophication, energy demands, waste disposal, and toxicity and radioactivity. The PC replacement ratio was found to be critical for savings in these categories; however, the amount of RCF in the mixture is limited by structural performance requirements on load-bearing masonry, and replacing more than 60 wt.% of PC with RCF could unacceptably compromise the integrity of the cementitious matrix. Due to this limitation, the use of RCF to produce blocks cannot be considered a 100% environmentally friendly solution, and the reuse of whole structural elements must be promoted to avoid the tolls associated with concrete recycling. In situations where the disposal of structural elements and concrete recycling is inevitable, the production of lightweight blocks according to the procedures outlined in this paper appears to be a feasible solution. However, alternative approaches to the use of SPs to increase the workability of fresh mortar should be sought to minimize ozone depletion and freshwater eutrophication.

It should be noted that the developed blocks share disadvantages with other cementitious highly-porous materials, e.g., relatively high water intake that negatively impacts the resistance to freeze-thaw degradation or poor resistance to concentrated force loads

Funding. This work was supported by the Czech Science Foundation, grant number 22-02702S (V. Nežerka and Z. Prošek) and by the Technology Agency of the Czech Republic, grant number S03010302 (J. Pešta and P. Tesárek).

References

ASTM E1876-01: Test method for dynamic youngs modulus, shear modulus, and poissons ratio by impulse excitation of vibration, 2006.

BS EN 12390-3:2009: Testing hardened concrete Part 3: Compressive strength of test specimens. British Standards Institution, London, 2009. doi: 10.3403/02508604u.

ASTM C215-14. Test method for fundamental transverse, longitudinal, and torsional resonant frequencies of concrete specimens, 2014.

A. Akhtar and A. K. Sarmah. Construction and demolition waste generation and properties of recycled aggregate concrete: A global perspective. *Journal of Cleaner Production*, 186:262–281, 2018. doi: 10.1016/j.jclepro.2018.03.085.

J. M. Allwood, M. F. Ashby, T. G. Gutowski, and E. Worrell. Material efficiency: A white paper. *Resources, Conservation and Recycling*, 55:362–381, 2011. doi: 10.1016/j.resconrec.2010.11.002.

ASTM C114. Standard Test Methods for Chemical Analysis of Hydraulic Cement. *Annual Book of ASTM Standards, ASTM International, West Conshohocken, PA*, 2018.

A. Barbudo, J. de Brito, L. Evangelista, M. Bravo, and F. Agrela. Influence of water-reducing admixtures on the mechanical performance of recycled concrete. *Journal of Cleaner Production*, 59:93–98, 2013. doi: 10.1016/j.jclepro.2013.06.022.

A. Bordy, A. Younsi, S. Aggoun, and B. Fiorio. Cement substitution by a recycled cement paste fine: Role of the residual anhydrous clinker. *Construction and Building Materials*, 132:1–8, 2017. doi: 10.1016/j.conbuildmat.2016.11.080.

M. Bravo, J. de Brito, L. Evangelista, and J. Pacheco. Durability and shrinkage of concrete with CDW as recycled aggregates: Benefits from superplasticizer's incorporation and influence of CDW composition. *Construction and Building Materials*, 168:818–830, 2018. doi: 10.1016/j.conbuildmat.2018.02.176.

J. Brožovský and Á. Dufka. Comparison of dynamic young's modulus of elasticity values measured by ultrasonic pulse and resonance methods. *Advanced Materials Research*, 1100:193–196, 2015. doi: 10.4028/www.scientific.net/amr.1100.193.

I. Carazeanu. Investigation of the hydration process in 3CaO·Al2O3-CaSO4·2H2O-plasticizer-H2O systems by X-ray diffraction. *Talanta*, 57:617–623, 2002. doi: 10.1016/s0039-9140(02)00100-5.

CEN. *EN 772-1:2011+A1:2015 - Methods of test for masonry units - Part 1: Determination of compressive strength*. CEN, Brussels (Belgium), accessed November 19, 2021.

CEN. *EN 15804:2012+A2:2019: Sustainability of construction works—Environmental product declarations—Core rules for the product category of construction products*. CEN, Brussels (Belgium), accessed November 27, 2020.

F. Colangelo, A. Forcina, I. Farina, and A. Petrillo. Life cycle assessment (LCA) of different kinds of concrete containing waste for sustainable construction. *Buildings*, 8:70, 2018. doi: 10.3390/buildings8050070.

E. COM. Roadmap to a resource efficient europe. *Communication from the Commission to European Parliament, the Council, the European Social and Economic Committee and the Committee of the Regions. Brussels: European Commission*, 2011.

E. COM. 398 final "towards a circular economy: A zero waste programme for europe". *Brussels*, 2, 2014.

E. Commission et al. Closing the loop—an eu action plan for the circular economy. *COM/2015/0614 final*, 2015.

S. R. da Silva and J. J. de Oliveira Andrade. Investigation of mechanical properties and carbonation of concretes with construction and demolition waste and fly ash. *Construction and Building Materials*, 153:704–715, 2017. doi: 10.1016/j.conbuildmat.2017.07.143.

T. Ding, J. Xiao, and V. W. Tam. A closed-loop life cycle assessment of recycled aggregate concrete utilization in China. *Waste Management*, 56:367–375, 2016. doi: 10.1016/j.wasman.2016.05.031.

T. Ding, J. Xiao, F. Qin, and Z. Duan. Mechanical behavior of 3d printed mortar with recycled sand at early ages. *Construction and Building Materials*, 248:118654, 2020. doi: 10.1016/j.conbuildmat.2020.118654.

Environdec. *The International EPD System*. https://www.environdec.com/home, accessed October 30, 2021.

M. R. Esa, A. Halog, and L. Rigamonti. Developing strategies for managing construction and demolition wastes in malaysia based on the concept of circular economy. *Journal of Material Cycles and Waste Management*, 19(3): 1144–1154, 2016. doi: 10.1007/s10163-016-0516-x.

European Committee for Standardization. *EN 197-1:2011: Cement. Composition, specifications and conformity criteria for common cements.* BSI, 2011.

European Committee for Standardization. *EN 196-2:2013: Method of testing cement. Chemical analysis of cement.* BSI, 2013.

European Standard EN 12350-5. Testing fresh concrete; flow table test. 2009.

L. Evangelista and J. de Brito. Concrete with fine recycled aggregates: a review. *European Journal of Environmental and Civil Engineering*, 18:129–172, 2013. doi: 10.1080/19648189.2013.851038.

M. Finkbeiner, A. Inaba, R. Tan, K. Christiansen, and H.-J. Klüppel. The new international standards for life cycle assessment: ISO 14040 and ISO 14044. *The International Journal of Life Cycle Assessment*, 11:80–85, 2006. doi: 10.1065/lca2006.02.002.

M. Florea, Z. Ning, and H. Brouwers. Activation of liberated concrete fines and their application in mortars. *Construction and Building Materials*, 50:1–12, 2014. doi: 10.1016/j.conbuildmat.2013.09.012.

Gabi Software. *Life Cycle Assessment LCA Software*. http://www.gabisoftware.com/, accessed October 30, 2020.

S. Ganesan, M. A. O. Mydin, M. Y. M. Yunos, and M. N. M. Nawi. Thermal properties of foamed concrete with various densities and additives at ambient temperature. *Applied Mechanics and Materials*, 747:230–233, 2015. doi: 10.4028/www.scientific.net/amm.747.230.

X. Gao, Q. Yu, and H. Brouwers. Reaction kinetics, gel character and strength of ambient temperature cured alkali activated slag–fly ash blends. *Construction and Building Materials*, 80:105–115, 2015. doi: 10.1016/j.conbuildmat.2015.01.065.

Gasbeton. *Environmental product declaration*. https://portal.environdec.com/api/api/v1/EPDLibrary/Files/d52c0010-ab02-4fd3-02f3-08d8f01e26c9/Data, accessed October 30, 2021.

D. Gastaldi, F. Canonico, L. Capelli, L. Buzzi, E. Boccaleri, and S. Irico. An investigation on the recycling of hydrated cement from concrete demolition waste. *Cement and Concrete Composites*, 61:29–35, 2015. doi: 10.1016/j.cemconcomp.2015.04.010.

A. Gholampour and T. Ozbakkaloglu. Performance of sustainable concretes containing very high volume class-f fly ash and ground granulated blast furnace slag. *Journal of Cleaner Production*, 162:1407–1417, 2017. doi: 10.1016/j.jclepro.2017.06.087.

M. D. González, P. P. Caballero, D. B. Fernández, M. M. J. Vidal, I. F. S. del Bosque, and C. M. Martínez. The design and development of recycled concretes in a circular economy using mixed construction and demolition waste. *Materials*, 14:4762, 2021. doi: 10.3390/ma14164762.

T. M. Grabois, G. C. Cordeiro, and R. D. T. Filho. The influence of recycled concrete and clay brick particles on the strength and porosity of cement-based pastes. In *RILEM Bookseries*, pages 189–194. 2017. doi: 10.1007/978-94-024-1207-9_30.

F. Han, S. Pu, Y. Zhou, H. Zhang, and Z. Zhang. Effect of ultrafine mineral admixtures on the rheological properties of fresh cement paste: A review. *Journal of Building Engineering*, 51:104313, 2022. doi: 10.1016/j.jobe.2022.104313.

M. U. Hossain, C. S. Poon, I. M. Lo, and J. C. Cheng. Comparative LCA on using waste materials in the cement industry: A hong kong case study. *Resources, Conservation and Recycling*, 120:199–208, 2017. doi: 10.1016/j.resconrec.2016.12.012.

S. Huysman, J. D. Schaepmeester, K. Ragaert, J. Dewulf, and S. D. Meester. Performance indicators for a circular economy: A case study on post-industrial plastic waste. *Resources, Conservation and Recycling*, 120:46–54, 2017. doi: 10.1016/j.resconrec.2017.01.013.

B. Karihaloo, A. Carpinteri, and M. Elices. Fracture mechanics of cement mortar and plain concrete. *Advanced Cement Based Materials*, 1:92–105, 1993. doi: 10.1016/1065-7355(93)90014-f.

J. Khatib. Properties of concrete incorporating fine recycled aggregate. *Cement and Concrete Research*, 35:763–769, 2005. doi: 10.1016/j.cemconres.2004.06.017.

A. Kleijer, S. Lasvaux, S. Citherlet, and M. Viviani. Product-specific life cycle assessment of ready mix concrete: Comparison between a recycled and an ordinary concrete. *Resources, Conservation and Recycling*, 122:210–218, 2017. doi: 10.1016/j.resconrec.2017.02.004.

C. Knoeri, E. Sanyé-Mengual, and H.-J. Althaus. Comparative LCA of recycled and conventional concrete for structural applications. *The International Journal of Life Cycle Assessment*, 18:909–918, 2013. doi: 10.1007/s11367-012-0544-2.

F. Krausmann, S. Gingrich, N. Eisenmenger, K.-H. Erb, H. Haberl, and M. Fischer-Kowalski. Growth in global materials use, GDP and population during the 20th century. *Ecological Economics*, 68:2696–2705, 2009. doi: 10.1016/j.ecolecon.2009.05.007.

T. Kupfer, C. M. Colodel, M. Kokborg, S. Schöll, M. Rudolf, L. Thellier, U. Bos, F. Bosch, M. Gonzalez, O. Schuller, J. Hengstler, A. Stoffregen, and D. Thylmann. *GaBi Database and Modelling Principles*. GaBi, 2020.

H. Lee, A. Hanif, M. Usman, J. Sim, and H. Oh. Performance evaluation of concrete incorporating glass powder and glass sludge wastes as supplementary cementing material. *Journal of Cleaner Production*, 170:683–693, 2018. doi: 10.1016/j.jclepro.2017.09.133.

Q. Liu, T. Tong, S. Liu, D. Yang, and Q. Yu. Investigation of using hybrid recycled powder from demolished concrete solids and clay bricks as a pozzolanic supplement for cement. *Construction and Building Materials*, 73:754–763, 2014. doi: 10.1016/j.conbuildmat.2014.09.066.

A. López-Uceda, J. Ayuso, M. López, J. Jimenez, F. Agrela, and M. Sierra. Properties of non-structural concrete made with mixed recycled aggregates and low cement content. *Materials*, 9:74, 2016. doi: 10.3390/ma9020074.

S. Lotfi and P. Rem. Recycling of end of life concrete fines (0–4 mm) from waste to valuable resources. In *High Tech Concrete: Where Technology and Engineering Meet*, pages 224–232. Springer International Publishing, 2017. doi: 10.1007/978-3-319-59471-2_28.

X. Ma and Z. Wang. Effect of ground waste concrete powder on cement properties. *Advances in Materials Science and Engineering*, 2013:1–5, 2013. doi: 10.1155/2013/918294.

S. K. Mangla, K. Govindan, and S. Luthra. Prioritizing the barriers to achieve sustainable consumption and production trends in supply chains using fuzzy analytical hierarchy process. *Journal of Cleaner Production*, 151:509–525, 2017. doi: 10.1016/j.jclepro.2017.02.099.

S. Marinković, J. Dragaš, I. Ignjatović, and N. Tošić. Environmental assessment of green concretes for structural use. *Journal of Cleaner Production*, 154:633–649, 2017. doi: 10.1016/j.jclepro.2017.04.015.

A. T. Marsh, A. P. Velenturf, and S. A. Bernal. Circular economy strategies for concrete: implementation and integration. *Journal of Cleaner Production*, 362:132486, 2022. doi: 10.1016/j.jclepro.2022.132486.

I. Martínez, M. Etxeberria, E. Pavón, and N. Díaz. Influence of demolition waste fine particles on the properties of recycled aggregate masonry mortar. *International Journal of Civil Engineering*, 16(9):1213–1226, 2018. doi: 10.1007/s40999-017-0280-x.

V. K. Mittal and K. S. Sangwan. Prioritizing barriers to green manufacturing: Environmental, social and economic perspectives. *Procedia CIRP*, 17:559–564, 2014a. doi: 10.1016/j.procir.2014.01.075.

V. K. Mittal and K. S. Sangwan. Fuzzy TOPSIS method for ranking barriers to environmentally conscious manufacturing implementation: government, industry and expert perspectives. *International Journal of Environmental Technology and Management*, 17:57, 2014b. doi: 10.1504/ijetm.2014.059466.

E. Namsone, G. Šahmenko, and A. Korjakins. Durability properties of high performance foamed concrete. *Procedia Engineering*, 172:760–767, 2017. doi: 10.1016/j.proeng.2017.02.120.

V. Nežerka, Z. Slížková, P. Tesárek, T. Plachý, D. Frankeová, and V. Petráňová. Comprehensive study on microstructure and mechanical properties of lime-pozzolan pastes. *Cement and Concrete Research*, 64:17–29, 2014. doi: 10.1016/j.cemconres.2014.06.006.

V. Nežerka, J. Zeman, and J. Němeček. Micromechanics-based simulations of compressive and tensile testing on lime-based mortars. *Mechanics of Materials*, 105:49–60, 2017. doi: 10.1016/j.mechmat.2016.11.011.

V. Nežerka, P. Havlásek, and J. Trejbal. Mitigating inclusion-induced shrinkage cracking in cementitious composites by incorporating recycled concrete fines. *Construction and Building Materials*, 248:118673, 2020. doi: 10.1016/j.conbuildmat.2020.118673.

V. Nežerka, P. Bílý, V. Hrbek, and J. Fládr. Impact of silica fume, fly ash, and metakaolin on the thickness and strength of the ITZ in concrete. *Cement and Concrete Composites*, 103:252–262, 2019. doi: 10.1016/j.cemconcomp.2019.05.012.

P. Niewiadomski, A. Karolak, D. Stefaniuk, A. Królicka, J. Szymanowski, and Ł. Sadowski. Cement paste mixture proportioning with particle packing theory: An ambiguous effect of microsilica. *Materials*, 14:6970, 2021. doi: 10.3390/ma14226970.

F. Özalp, H. D. Yılmaz, M. Kara, Ömer Kaya, and A. Şahin. Effects of recycled aggregates from construction and demolition wastes on mechanical and permeability properties of paving stone, kerb and concrete pipes. *Construction and Building Materials*, 110:17–23, 2016. doi: 10.1016/j.conbuildmat.2016.01.030.

F. Pacheco-Torgal. Introduction to advances in construction and demolition waste. In *Advances in Construction and Demolition Waste Recycling*, pages 1–10. Elsevier, 2020. doi: 10.1016/b978-0-12-819055-5.00001-2.

J. M. Paris, J. G. Roessler, C. C. Ferraro, H. D. DeFord, and T. G. Townsend. A review of waste products utilized as supplements to portland cement in concrete. *Journal of Cleaner Production*, 121:1–18, 2016. doi: 10.1016/j.jclepro.2016.02.013.

J. Pešta, T. Pavlů, K. Fořtová, and V. Kočí. Sustainable masonry made from recycled aggregates: LCA case study. *Sustainability*, 12:1581, 2020. doi: 10.3390/su12041581.

Z. Prošek, V. Nežerka, R. Hlůžek, J. Trejbal, P. Tesárek, and G. Karra'a. Role of lime, fly ash, and slag in cement pastes containing recycled concrete fines. *Construction and Building Materials*, 201:702–714, 2019. doi: 10.1016/j.conbuildmat.2018.12.227.

Z. Prošek, V. Nežerka, and P. Tesárek. Enhancing cementitious pastes with waste marble sludge. *Construction and Building Materials*, 255:119372, 2020a. doi: 10.1016/j.conbuildmat.2020.119372.

Z. Prošek, J. Trejbal, V. Nežerka, V. Goliáš, M. Faltus, and P. Tesárek. Recovery of residual anhydrous clinker in finely ground recycled concrete. *Resources, Conservation and Recycling*, 155:104640, 2020b. doi: 10.1016/j.resconrec.2019.104640.

H. Quan and H. Kasami. Experimental study on the effects of recycled concrete powder on properties of self-compacting concrete. *The Open Civil Engineering Journal*, 12:430–440, 2018. doi: 10.2174/1874149501812010430.

A. Raj, D. Sathyan, and K. Mini. Physical and functional characteristics of foam concrete: A review. *Construction and Building Materials*, 221:787–799, 2019. doi: 10.1016/j.conbuildmat.2019.06.052.

B. Raj, D. Sathyan, M. K. Madhavan, and A. Raj. Mechanical and durability properties of hybrid fiber reinforced foam concrete. *Construction and Building Materials*, 245:118373, 2020. doi: 10.1016/j.conbuildmat.2020.118373.

I. Rhee, J. S. Lee, and Y.-S. Roh. Fracture parameters of cement mortar with different structural dimensions under the direct tension test. *Materials*, 12:1850, 2019. doi: 10.3390/ma12111850.

K. L. Scrivener, V. M. John, and E. M. Gartner. Eco-efficient cements: Potential economically viable solutions for a low-CO2 cement-based materials industry. *Cement and Concrete Research*, 114:2–26, 2018. doi: 10.1016/j.cemconres.2018.03.015.

R. Serpell and M. Lopez. Reactivated cementitious materials from hydrated cement paste wastes. *Cement and Concrete Composites*, 39:104–114, 2013. doi: 10.1016/j.cemconcomp.2013.03.020.

M. Shojaei, K. Behfarnia, and R. Mohebi. Application of alkali-activated slag concrete in railway sleepers. *Materials & Design*, 69:89–95, 2015. doi: 10.1016/j.matdes.2014.12.051.

Z. Shui, D. Xuan, H. Wan, and B. Cao. Rehydration reactivity of recycled mortar from concrete waste experienced to thermal treatment. *Construction and Building Materials*, 22:1723–1729, 2008. doi: 10.1016/j.conbuildmat.2007.05.012.

V. Sousa and J. A. Bogas. Comparison of energy consumption and carbon emissions from clinker and recycled cement production. *Journal of Cleaner Production*, 306:127277, 2021. doi: 10.1016/j.jclepro.2021.127277.

V. Sousa, J. A. Bogas, S. Real, and I. Meireles. Industrial production of recycled cement: energy consumption and carbon dioxide emission estimation. *Environmental Science and Pollution Research*, 255:119372, 2022. doi: 10.1007/s11356-022-20887-7.

A. Steshenko, A. Kudyakov, V. Konusheva, and O. Syrkin. Structure formation control of foam concrete. *AIP Conference Proceedings*, 1800:020001, 2017. doi: 10.1063/1.4973017.

P. C. Strange and A. H. Bryant. The role of aggregate in the fracture of concrete. *Journal of Materials Science*, 14: 1863–1868, 1979. doi: 10.1007/bf00551025.

J. Topič, J. Fládr, and Z. Prošek. Flexural and compressive strength of the cement paste with recycled concrete powder. *Advanced Materials Research*, 1144:65–69, mar 2017. doi: 10.4028/www.scientific.net/amr.1144.65. URL https://doi.org/10.4028%2Fwww.scientific.net%2Famr.1144.65.

J. Topič, Z. Prošek, J. Fládr, and P. Tesárek. Vliv jemnosti recyklované betonové moučky na vỳvin hydratačního tepla a vliv jejího množství na mechanicko-fyzikální vlastnosti cementové pasty. In *Waste Forum*, volume 2, pages 268–274, 2018.

J. Turk, Z. Cotič, A. Mladenovič, and A. Šajna. Environmental evaluation of green concretes versus conventional concrete by means of LCA. *Waste Management*, 45:194–205, 2015. doi: 10.1016/j.wasman.2015.06.035.

L. K. Turner and F. G. Collins. Carbon dioxide equivalent (CO2-e) emissions: A comparison between geopolymer and OPC cement concrete. *Construction and Building Materials*, 43:125–130, 2013. doi: 10.1016/j.conbuildmat.2013.01.023.

US Geological Survey & Orienteering S and US Geological Survey. *Mineral Commodity Summaries, 2009*. Government Printing Office, 2009.

H. Van Damme. Concrete material science: Past, present, and future innovations. *Cement and Concrete Research*, 112:5–24, 2018. doi: 10.1016/j.cemconres.2018.05.002.

D. R. Vieira, J. L. Calmon, and F. Z. Coelho. Life cycle assessment (LCA) applied to the manufacturing of common and ecological concrete: A review. *Construction and Building Materials*, 124:656–666, 2016. doi: 10.1016/j.conbuildmat.2016.07.125.

Y. A. Villagrán-Zaccardi, A. T. Marsh, M. E. Sosa, C. J. Zega, N. De Belie, and S. A. Bernal. Complete re-utilization of waste concretes–valorisation pathways and research needs. *Resources, Conservation and Recycling*, 177:105955, 2022. doi: 10.1016/j.resconrec.2021.105955.

L. Wang, J. Wang, H. Wang, Y. Fang, W. Shen, P. Chen, and Y. Xu. Eco-friendly treatment of recycled concrete fines as supplementary cementitious materials. *Construction and Building Materials*, 322:126491, 2022. doi: 10.1016/j.conbuildmat.2022.126491.

J. Xiao. *Recycled Aggregate Concrete Structures*. Springer Berlin Heidelberg, 2018. doi: 10.1007/978-3-662-53987-3.

D. Zou, Z. Que, W. Cui, X. Wang, Y. Guo, and S. Zhang. Feasibility of recycling autoclaved aerated concrete waste for partial sand replacement in mortar. *Journal of Building Engineering*, 52:104481, 2022. doi: 10.1016/j.jobe.2022.104481.

S. Zou, J. Xiao, T. Ding, Z. Duan, and Q. Zhang. Printability and advantages of 3d printing mortar with 100% recycled sand. *Construction and Building Materials*, 273:121699, 2021. doi: 10.1016/j.conbuildmat.2020.121699.